Nuclear Instruments and Methods in Physics Research A 648 (2011) S269–S272

Contents lists available at ScienceDirect

Nuclear Instruments and Methods in Physics Research A

journal homepage: www.elsevier.com/locate/nima

Simulation and measurement of grating-based X-ray phase-contrast imaging

P. Bartl [a,*], F. Bayer [a], J. Durst [a], W. Haas [a,b], T. Michel [a], G. Pelzer [a], A. Ritter [a], T. Weber [a], G. Anton [a]

[a] University of Erlangen-Nuremberg, ECAP - Erlangen Centre for Astroparticle Physics, Erwin-Rommel-Str. 1, 91058 Erlangen, Germany
[b] University of Erlangen-Nuremberg, Pattern Recognition Lab, Martenstr. 3, 91058 Erlangen, Germany

ARTICLE INFO

Available online 21 November 2010

Keywords:
Phase contrast
Grating-based interferometry
X-ray imaging
Photon-counting detector
Medipix
Simulation of X-rays

ABSTRACT

In this paper we present results from simulations on grating-based phase contrast imaging. Herein, the performance of a grating-based interferometer concerning the X-ray's energy is shown. Additionally, geometric parameters of the interferometer were investigated. In the experimental part of this work we present the dependency of the Talbot-Lau interferometer setup on the lower energy threshold of the Medipix-detector. These are the first energy sensitive measurements acquired within the applied method. Furthermore, we demonstrate the difference between a differential and an integral measurement by comparing the phase and absorption image. The conclusion of this work is the detailed characterisation of grating-based phase contrast imaging regarding its energy dependent behaviour and geometric parameters of the gratings.

1. X-ray grating-based interferometry

Grating-based interferometry with X-rays has been applied to synchrotron facilities since more than a decade [1–4]. Several years ago phase-contrast imaging using a Talbot-Lau interferometer was introduced on table-top experimental setups [5–8]. The quest of current science of this method is its optimisation and the search for new applications in the field of conventional X-ray imaging. The grating interferometer is based on the Talbot effect [9]. A scheme of the interferometer can be found in Fig. 3 in Section 3.1. According to this effect, a periodic interference pattern is generated in a certain fractional Talbot distance d_T, when a (phase) grating is placed into a coherent radiation field. A local lateral shift d_Φ of the periodic intensity fringes occurs if the wavefront is deviated by an object placed inside this field. By determining this shift d_Φ to the reference pattern without the object in the radiation field the wavenfront's phase gradient $\partial\Phi/\partial x$ can be reconstructed by

$$\frac{d_\Phi}{d_T} = \frac{1}{k}\cdot\frac{\partial\Phi}{\partial x} \tag{1}$$

where k denotes the wavenumber. The relative absorption in the grating-based setup is calculated by the ratio of the mean intensity measured with object and without object. Additionally, the darkfield value can be defined by the ratio of the two acquired visibilities with object and without object. The visibility V itself is calculated as the contrast of the interference fringes by e.g. Ref. [10]

$$V = \frac{I_{max}-I_{min}}{I_{max}+I_{min}}. \tag{2}$$

I_{max} and I_{min} denote the maximum and minimum intensity of the fringes. The visibility is a quantity to assess the quality of the interferometer.

2. Simulation of grating-based phase contrast imaging

In order to calculate X-ray phase contrast imaging we developed in our group a simulation framework, which is based on a wave propagation and a Monte Carlo part [11,12]. Each of the parts considers the corresponding physical aspect of the photon. For the purpose of this paper it is sufficient to take the wave propagation into account. The following subsections show numerical results on different grating simulations.

2.1. Simulation of the phase grating

The visibility (see Eq. (2)) is an important quantity in order to characterise the quality of a grating-based interferometer. Additionally, the energy dependency of the Talbot effect plays a strong role for this imaging approach. For this reason we investigated the energy dependency of the visibility. As a further parameter to optimise the setup the duty cycle d of the grating was chosen. It is defined as the ratio of the width of the grating bars d_G and the period of the grating p_G: $d = d_G/p_G$. Thus, its values vary from zero to one.

Fig. 1 shows the simulated result, in which the visibility was calculated while scanning the energy and the duty cycle of the phase grating G1. Further parameters defining the setup were a period of G1 of $p_{G1} = 5\ \mu m$ and a height of $h_{G1} = 14\ \mu m$ corresponding to a design-energy of $E_D = 40$ keV ($\pi-$phase$-$shift in the wavefront). The analyser grating was assumed to consist of gold bars with a height

* Corresponding author.
E-mail address: peter.bartl@physik.uni-erlangen.de (P. Bartl).

0168-9002/$ - see front matter © 2010 Elsevier B.V. All rights reserved.
doi:10.1016/j.nima.2010.11.061

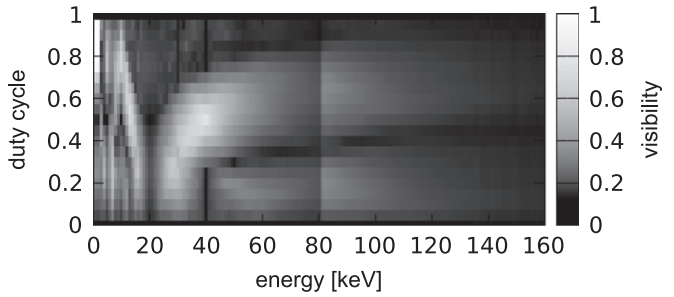

Fig. 1. Dependency of the visibility of the phase grating on the X-ray energy and the duty cycle. The design-energy was 40 keV.

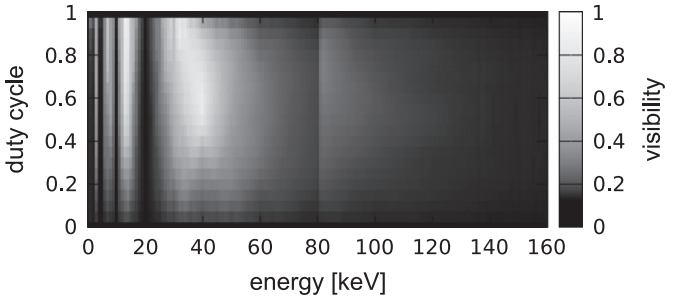

Fig. 2. Dependency of the visibility of the analyser grating on the X-ray energy and the duty cycle. The design-energy was 40 keV.

of $h_{G2} = 120\ \mu m$, a period of $p_{G2} = 2.5\ \mu m$, and a duty cycle of $d_{G2} = 0.5$. The visibility V in Fig. 1 shows a maximum value at $E_D = 40$ keV and $d_{G1} = 0.5$. It decreases for energies higher than $E_D = 40$ keV and $d \neq 0.5$. At an energy of 82 keV, which corresponds to the K'' absorption edge of the gold bars of the analyser grating a step to higher visibilities occurs. At lower energies than $E_D = 40$ keV a mix of maxima and minima is observed. The reason for this is, that for certain combinations of energy and duty cycle conditions for the fractional Talbot effect are met. A detailed description to this can be found in [13]. A phase shift of π for example occurs for $E = E_D/(2n+1)$ and an effective phase shift of zero for $E = E_D/(2n)$, where n is an integer.

2.2. Simulation of the analyser grating

The equivalent calculation of Section 2.1 was done for the dependency of the analyser grating. This means that d_{G1} was fixed to 0.5. Fig. 2 demonstrates, that the result of this simulation is similar to the result of Fig. 1. The maximum values of visibility with respect to the energy can be found at $E = E_D/(2n+1)$ with $n \in \mathbb{N}_0$. In contrast to Fig. 1 an increasing duty cycle leads in Fig. 2 to a slighter decrease or even to an increase of the visibility. It should be remarked at this point, that for applications that have to deal with dose deposition, an increasing d_{G2} leads to higher dose deposition in the analyser grating.

3. Measurement of grating-based phase contrast imaging

3.1. Experimental setup

The grating-based interferometer setup consists of a microfocus X-ray tube, a phase grating G1, and an analyser grating G2 (see scheme in Fig. 3). The phantom we used was a stepped wedge. It consists of PMMA and the step height is 2 mm with a step length of 5 mm. The bottom line of the object has an angle of 1.08 rad with the x-axis, as indicated in Fig. 3. This leads in the detection plane to a projected ratio of step width and length of 0.8. As detection device

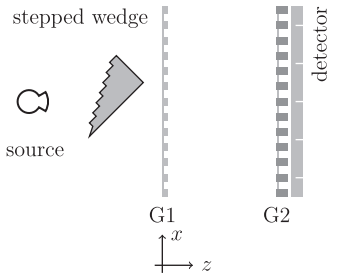

Fig. 3. Schematic drawing of the experimental setup with a stepped wedge. In the real experiment the wedge overlaps more than the detective area.

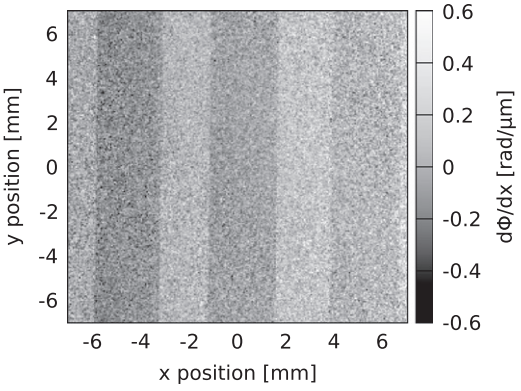

Fig. 4. Differential phase image of the stepped wedge.

we used the photon counting Medipix-detector [14]. The gratings were fabricated at the Karlsruhe Institute of Technology (KIT, www.kit.edu). G1 was made of nickel with a height of 14.1 µm corresponding to an approximate phase shift of π for 40 keV design-energy.

The analyser grating G2 was fabricated of 120 µm gold to achieve sufficient absorption. Both gratings had a period of 5 µm. The total length of the setup was calculated to $d_{Source-G1} + d_{G1-G2} = 40.32$ cm [15]. The phase stepping technique to acquire the datasets (described e.g. in [16]) was applied over one interference fringe period taking eight phase steps. The used X-ray spectrum was a 70 kV tungsten spectrum of a microfocus tube with an additional filter of 1 mm alumimium. The Medipix-detector had a pixelpitch of 55 µm and its lower energy threshold was set to 5.2 keV.

3.2. Differential and integral imaging

Figs. 4 and 5 show as an example the phase and absorption image as they were reconstructed from the experiment. The difference between the phase and the absorption information is significant. The sawtooth-like profile of the stepped wedge becomes in the differential (phase) image visible through dark and bright stripes (see Fig. 4). The thickness variation of the wedge profile can be observed as a global trend over the image as well. This behaviour is also clearly visible in the integral (absorption) image in Fig. 5. The single steps of the phantom are hardly visible, however.

In order to demonstrate the difference between the phase and the absorption information linescans were drawn through both images. After that the phase profile was numerically integrated and the absorption profile numerically deviated. Figs. 6 and 7 show the according differential and integral profiles in comparison. In order to decrease statistical and systematical fluctuations the linescans were averaged over 200 detector lines. The differential phase values were arbitrarily shifted to give only positive values. This was done to avoid artefacts in the later on integrated linescan (see Fig. 7). As the acquired